



# International Journal of Sciences: Basic and Applied Research (IJSBAR)

ISSN 2307-4531  
(Print & Online)

<http://gssrr.org/index.php?journal=JournalOfBasicAndApplied>



---

## Lateral Rock Property Prediction by Post Stack Acoustic Impedance Inversion: A Case Study from Offshore Niger Delta

Difference Odeyovwi Ogagarue<sup>a\*</sup>, God'swill Igoni Alaminikuma<sup>b</sup>

<sup>a</sup>*Department of Earth Sciences, Federal University of Petroleum Resources, Effurun, Nigeria*

<sup>b</sup>*Department of Earth Sciences, Federal University of Petroleum Resources, Effurun, Nigeria*

<sup>a</sup>*Email: ogagarue.odeyovwi@fupre.edu.ng*

### Abstract

A post stack acoustic impedance seismic inversion study was carried out by integrating well logs and 3D seismic data obtained in a Niger Delta offshore field. The aim was to delineate lateral variations in subsurface rock properties especially lithology and density, which could aid in petrophysical and facies modeling to constrain the extent of hydrocarbon zones in the development of the field. Log data comprising GR, density and compressional sonic logs from one well, and a 5 – 18 degree angle stack of approximately 43.05 sq.km 3D PTSM dataset were used for the study. A deterministic model-driven inversion workflow that includes forward modeling of reflection coefficients from a low frequency impedance model derived from the well logs and convolution of the reflection coefficients with a source wavelet derived from the seismic and well log data was adopted for the study. Density and acoustic impedance volumes obtained from the inversion reveal the reservoir top at the well location, and show lateral variations in these properties away from well control. The results obtained are important for accurate structural and stratigraphic interpretation to reduce the risk of exploratory and development well locations in the field.

**Keywords:** Acoustic impedance; Seismic inversion; Deterministic; Model-driven; Interpretation.

---

\* Corresponding author.

## 1. Introduction

A detailed understanding of reservoir rock properties is important for reducing the ambiguities and uncertainties associated with reservoir characterization for optimized hydrocarbon recovery. Seismic reflection data are interface properties which result from acoustic impedance contrast at interfaces between layers. Post stack acoustic impedance inversion aims to transform the interface-based seismic data into acoustic impedance of the respective geologic layers [1,2], providing useful information for quantitative estimates of summary reservoir properties such as average porosity, net-to-gross and other parameters [3]. The process attempts to extract subsurface geology from the input seismic data. In particular, the layer-based acoustic impedance derived makes it possible for lithology, porosity, fluid content and other petrophysical parameters to be interpreted in a lateral sense over an area thereby providing a measure of refinement of structural interpretation and reservoir geometry, including rock property prediction and reservoir characterization. Seismic inversion has the additional benefit of greatly improving interpretation efficiency [4].

Post-stack acoustic impedance inversion is based on the acoustic theory, and different inversion methods such as model based, band-limited and the sparse spike are in the literature for carrying out seismic inversion [5,6,7,8,9]. The model-based post stack acoustic impedance inversion technique was adopted in this study, and the implementation is based on the generalized linear inversion (GLI) described by [9]. The generalized linear inversion is based on utilizing the Taylor series expansion:

$$S(M) = S(M_1) + \frac{\partial S(M_1)}{\partial M} \Delta M + \dots \quad (1)$$

where,

$M_1$  = initial model

$M$  = "true model"

$\Delta M$  = change in model parameters

$S(M)$  = observed seismic

$S(M_1)$  = synthetic seismic from initial model

The success of the model-based inversion is the ability to minimize the difference ( $\Delta S$ ) between the observed seismic  $S(M)$  and synthetic seismic  $S(M_1)$  derived from the initial model. The acoustic impedance model which gives the minimum error between the real and synthetic seismic data after several iterations of the inversion sequence is retained as the solution. To obtain the error, Equation (1) is truncated to the first order and solved for  $\Delta M$ :

$$S(M) - S(M_1) = \frac{\partial S(M_1)}{\partial M} \Delta M \quad (2)$$

$\Delta S$  is defined as:

$$\Delta S = S(M) - S(M_i) = \frac{\partial S(M_i)}{\partial M} \Delta M = L \Delta M \quad (3)$$

where  $L$  is a matrix of derivatives. The solution is the least squares fit [10]:

$$\Delta M = (L^T L)^{-1} L^T \Delta S \quad (4)$$

Equation (4) requires a stable inverse to get a perfect fit, but this may not always be the case because there is a noise component in  $\Delta S$  similar to the noise in the seismic data. To stabilize the solution, a pre-whitening factor is introduced [11], given by:

$$\Delta M = (L^T L + \lambda I)^{-1} L^T \Delta S \quad (5)$$

where,

$\lambda$  = pre - whitening factor

$I$  = identity matrix

In the application of the GLI technique, the earth is assumed to be one-dimensional, comprising a series of layers, each layer having a “blocky” acoustic impedance profile. The initial guess of the acoustic impedance profile is the impedance log that has been interpolated for the entire survey guided by horizon interpretation [12], and the model is related to the observed seismic by the convolutional model, given by:

$$S(t) = W(t) * r(t) + n(t) \quad (6)$$

where,

$S(t)$  = seismic trace

$W(t)$  = seismic wavelet

$r(t)$  = 1-D earth reflectivity

$n(t)$  = additive noise

$t$  = time

Assuming the data is noise free or of high signal-to-noise ratio as would be the case for an ideal pre-stack time migrated data, Equation (6) is reduced to:

$$S(t) = W(t) * r(t) \quad (7)$$

Mathematically, the reflectivity or reflection coefficient  $r(t)$  at an interface between two layers  $i$  and  $i + 1$  above and below the interface, respectively, is given by:

$$r = \frac{Z_{i+1} - Z_i}{Z_{i+1} + Z_i} \quad (8)$$

where  $Z$  is acoustic impedance, given by:

$$\begin{aligned} Z_{i+1} &= \rho_{i+1} V_{i+1} \\ Z_i &= \rho_i V_i \end{aligned} \quad (9)$$

and  $\rho$  and  $V$  are density and velocity of the layers.

In seismic inversion, the objective is to solve Equation (7) to obtain the earth's reflectivity function,  $r(t)$ , which is then related to the impedance. Using Equation (8), the impedance in layer  $i + 1$  is given by:

$$Z_{i+1} = Z_i \left[ \frac{1+r}{1-r} \right] \quad (10)$$

Equation (10) implies that by knowing the reflection coefficient,  $r$  between two layers, and the acoustic impedance of the upper layer,  $Z_i$ , the acoustic impedance of the deeper layer  $Z_{i+1}$  can be obtained. The acoustic impedance of layer  $i$  is derived recursively from impulse response  $r_j$  using Equation 11):

$$Z_i = Z_1 \prod_{j=2}^i \left[ \frac{1+r_j}{1-r_j} \right] \quad (11)$$

where the impedance of the uppermost layer,  $Z_1$  needs to be input to start the recursion [13]. Solving Equation (7) for  $r(t)$  entails deconvolution such that when the seismic trace  $S(t)$  is convolved with an inverse filter,  $f(t)$ , the wavelet  $W(t)$  is effectively removed or compressed, leaving ideally the reflectivity  $r(t)$  series:

$$r(t) = S(t) * f(t) \quad (12)$$

Using Equation (13) in Equation (7) gives:

$$S(t) = W(t) * S(t) * f(t) \quad (13)$$

Eliminating  $S(t)$  from both sides, gives:

$$\delta(t) = W(t) * f(t) \tag{14}$$

where  $\delta(t)$  is Kronecha delta function defined by:

$$\delta(t) = \begin{cases} 1 & t=0 \\ 0 & \text{elsewhere} \end{cases} \tag{15}$$

Based on Equation (15), the filter operator  $f(t)$  required to obtain the earth's reflectivity  $r(t)$  from the observed seismogram  $S(t)$ , is therefore the mathematical inverse of the source wavelet such that:

$$\begin{aligned} S(t) &= W(t) * r(t) * \frac{1}{W(t)} \\ &= \frac{W(t)}{W(t)} * r(t) \end{aligned} \tag{16}$$

From the foregoing, post stack seismic inversion equations suggest that if the additive noise component is removed or reduced from the recorded seismogram, the input wavelet deconvolved to reverse convolution in order to restore the original wave shape, we would be left with the reflectivity series which could then be related to acoustic impedance.

In this study, the model-based inversion technique was carried out to invert post stack 3D seismic volume acquired in the Niger Delta offshore for acoustic impedance with the intent to determine lateral variations in lithology and pay zones away from well locations. Seismic data is band-limited and typical low-frequencies that would be required to obtain reasonable impedance through inversion are absent from the seismic data [14]. The low-frequency impedance information missing from the seismic data is derived from well logs.

### ***1.1. Location and Geology***

The study area is located in the southeastern part of the Niger Delta offshore, at water depths ranging from 750 m to 850 m (Figure 1). The Niger Delta is one of the world's largest and sandiest basins, situated on the West African continental margin at the apex of the Gulf of Guinea [15]. It lies between latitudes 4<sup>0</sup>N and 6<sup>0</sup>N and longitudes 3<sup>0</sup>E and 9<sup>0</sup>E, and covers a surface area of approximately 75,000 sq. km. The delta ranges in thickness from 10 km to 12 km, extending more than 300 km from apex to mouth, and comprising a series of thick, shore parallel, southward-migrating depositional sub-basins (depobelts) with significant temporal and spatial connotations. It is sub-divided into three lithostratigraphic sequences namely the Benin, Agbada and Akata Formations [16,17,18]. The Benin Formation consists of massive deposits of mainly alluvial and upper coastal plain sands with a few minor shale interbeds. The Agbada Formation consists of alternating sandstones and shales, the upper part having more sandstone content than the lower part. The Agbada Formation represents the

delta front, distributary channels and delta plain, with the sandy part being regarded as the main hydrocarbon reservoir in the Niger Delta. The Akata Formation is the basal unit of the Tertiary Niger Delta complex, and is composed predominantly of medium to hard, dark grey shales with plant remains especially at its upper part. The Tertiary Niger Delta has been identified as the only petroleum system in the Nigeria Delta, and comprises the Akata shales and shales at the base of the Agbada Formation.

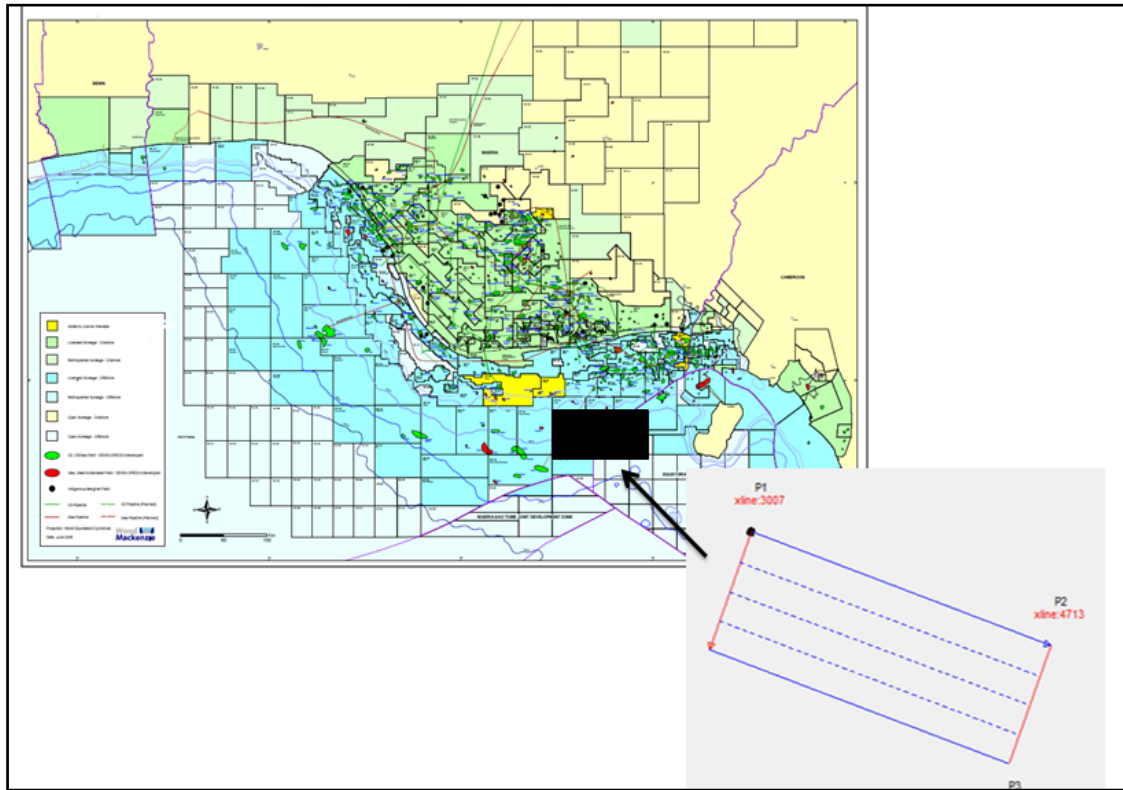


**Figure 1:** Concession map of the Niger Delta showing the study area and seismic data acquisition geometry

## 2. Materials and Methods

### 2.1. Materials

The data utilized for this study comprise a  $5^{\circ} - 18^{\circ}$  near angle stack of approximately 43.21 sq. km 3D PSTM seismic dataset obtained from an offshore field in the Niger Delta. The field contains two wells coded W-XXX and W-YYY, and both wells contain GR, density, compressional and shear sonic log measurements. The wells are 4 km apart. Checkshot data was available in well W-XXX. The seismic volume consists of 324 inlines and 1,707 crosslines, spaced 12.5 m and 6.25 m, respectively giving approximate survey size of 43.05 sq.km. The seismic survey grid and well location map of the area is shown in Figure 2, and well data from W-XXX is shown in Figure 3.

### 2.2. Checkshot Correction and Well-to-seismic tie

Due to uncertainties, the P-wave log rarely matches the two-way travel time on the seismic and as such, the first task carried out was checkshot correction of the compressional sonic log. Next, a well-to-seismic tie was carried

out to obtain a correction for the compressional sonic at the well locations. To achieve this, a statistical least squares approach was utilized to estimate an initial zero-phased, symmetrical wavelet of length 180 ms and frequency 45 Hz from an autocorrelation function of the seismic data alone, using four (4) seismic traces on both sides of each well.

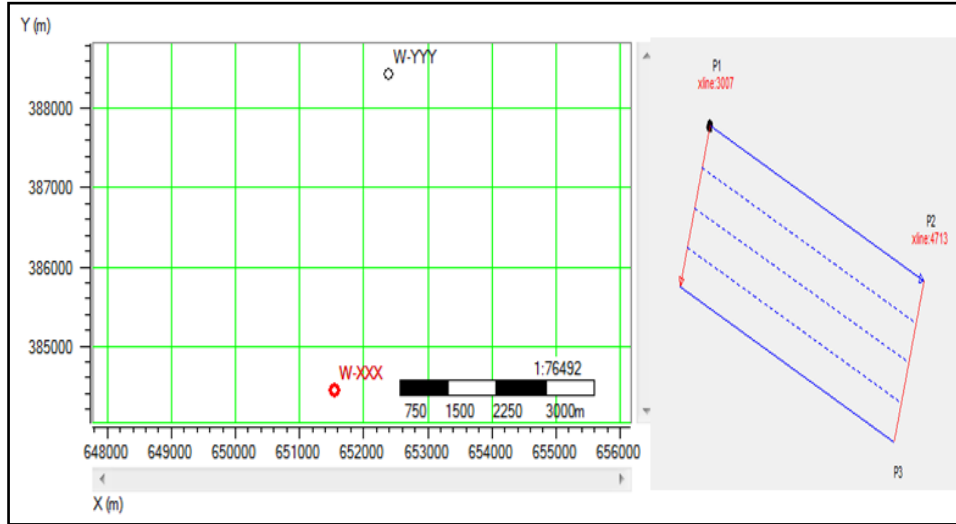


**Figure 2:** Well location map and seismic survey grid of the study area.

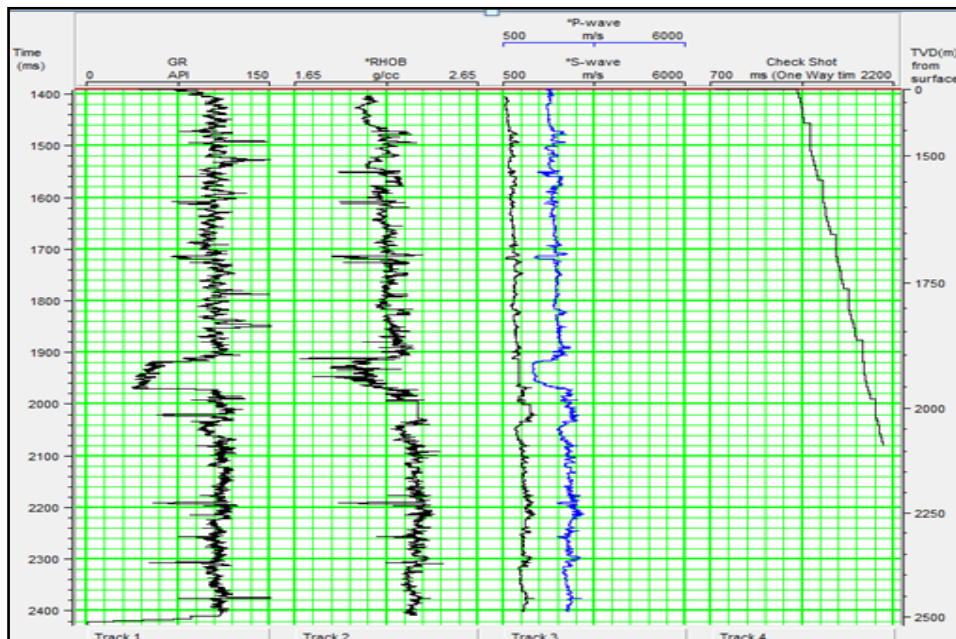


**Figure 3:** Well log data from well W-XXX: Track 1(GR); Track 2 (measured bulk density Log; Track 3 (measured compressional and shear sonic logs); Track 4 (checkshot).

A synthetic seismogram was thereafter generated by convolution of the wavelet and earth's reflectivity function, obtained from the P-wave velocity and density logs. The synthetic seismogram was correlated to the composite trace, which is the average seismic traces around the well location; the maximum coefficient of correlation

obtained was 45%. A new P-wave velocity log was created, and using a combination of this new log and the seismic data, a model wavelet was derived which matched the amplitude, frequency and phase characteristics of the seismic data, improving the correlation coefficient to 58%. Figure 4 shows the correlation plots for the statistical and combined wavelet estimation, and the final well-to-seismic correlation.

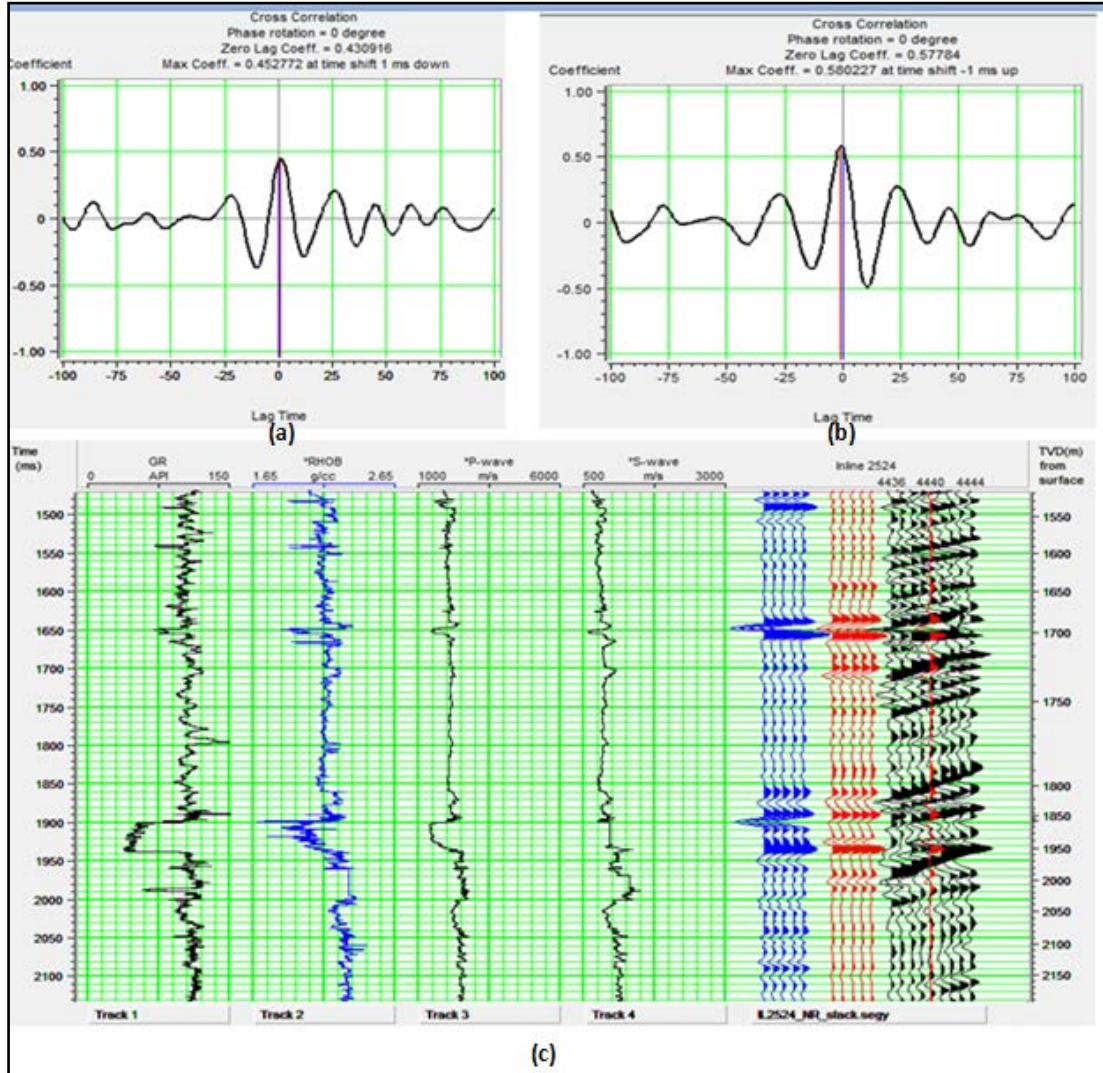


**Figure 4:** Well-to-seismic correlation: (a) correlation plot based on seismic data alone (b) correlation plot from well and seismic combination (c) final well-to-seismic Correlation display: synthetic seismic traces (blue); composite seismic traces (red); Field seismic traces (black).

### 2.3. Initial P-Impedance Model, Model Analysis and Inversion

The initial P-impedance model was built using the P-impedance logs calculated at the two well locations. The input P-wave log for the P-impedance log calculation at well-XXX was the new sonic log derived from correlation of the well to seismic. The calculated P-impedance logs were filtered with a 10/15 Hz low-pass filter to retain only the low frequencies not present in the seismic data; this provided the background trend information for the inversion. In this study, six horizons were picked on the basis of prominent amplitudes and



these provided prior geological information for the initial model such as thickness and acoustic impedance of the layers. Due to the distance separating the wells, the method of ‘inverse distance weighted’ was used to interpolate the impedance information from trace to trace away from the wells to other parts of the entire survey, guided by the picked horizons. Finally, a model-based inversion analysis was carried out on the initial model at well W-XXX to evaluate the accuracy of the inversion and following from this, a post stack inversion was performed on the entire data volume.

### 3. Results and Discussion

Figure 5 shows the initial P-impedance model at inline 2524 with inserted corrected P-wave velocity log at well W-XXX. The colour variation in the model shows amplitudes that correspond to P-impedance, ranging from 10891 to about 21866  $\text{m/s}^*\text{g/cm}^3$  and having a general increase with depth trend.

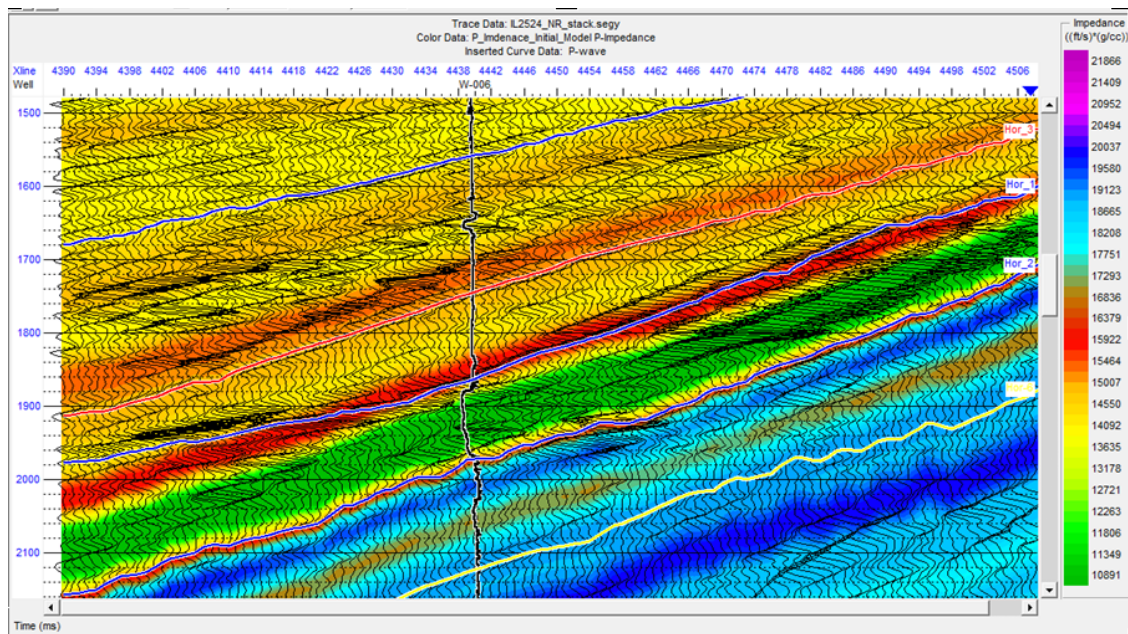
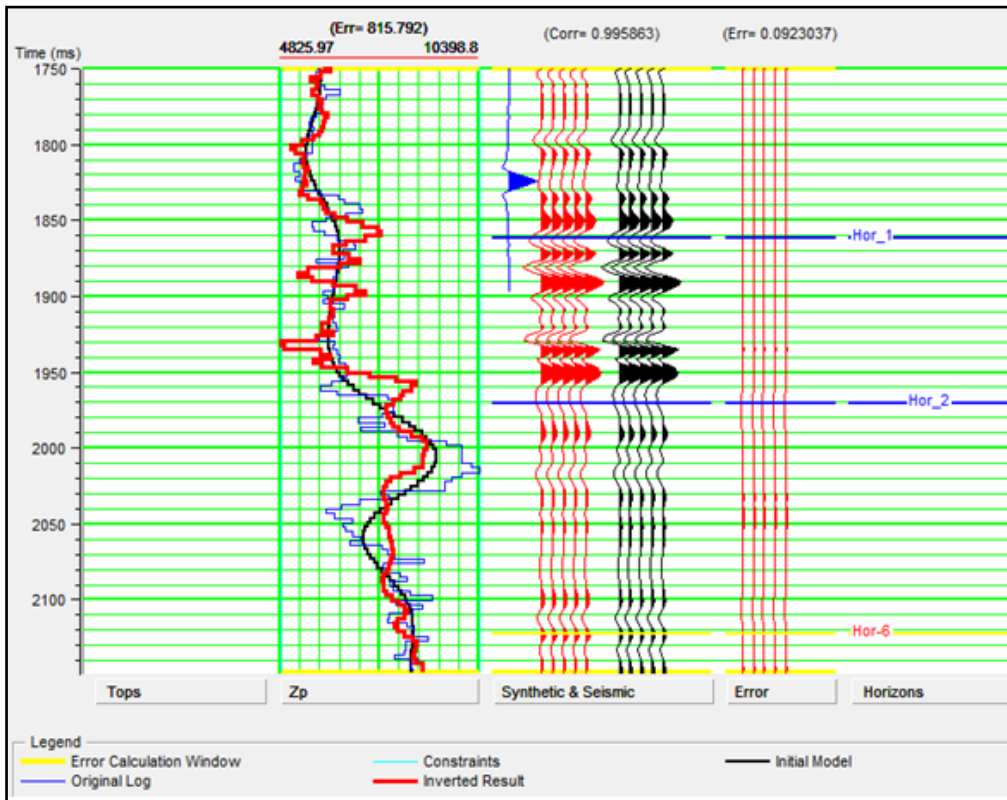


**Figure 5:** Initial background P-impedance model at inline 2524 showing well W-XXX location and inserted corrected P-wave velocity log from the well.

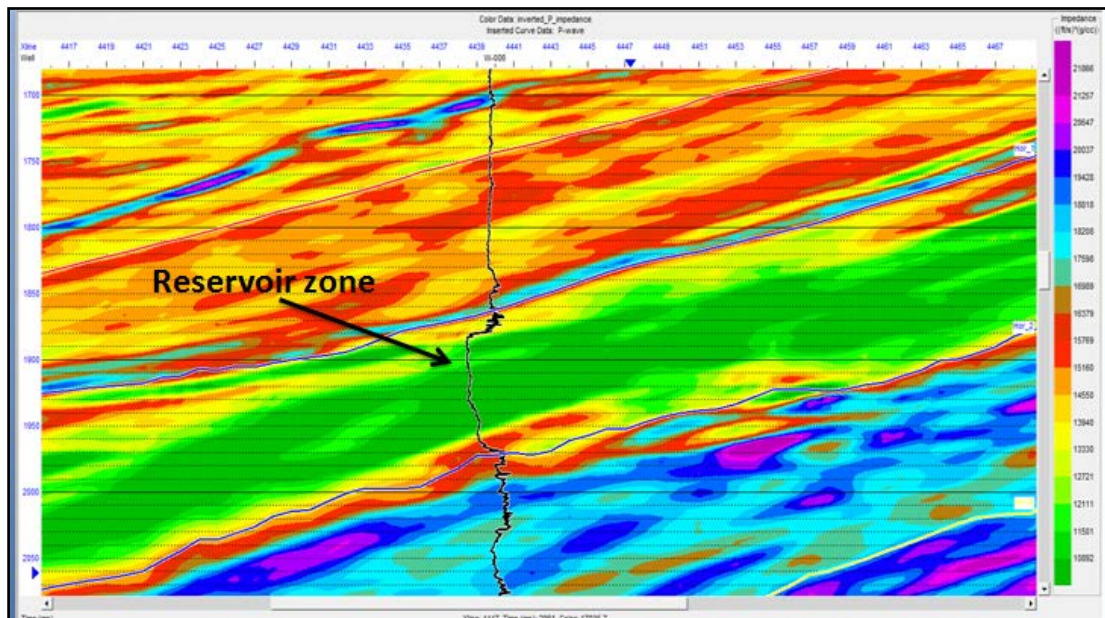
Figure 6 shows the inversion analysis result at this well location. The synthetic (red) and seismic trace (black) correlated well at the well location, giving a near perfect correlation (correlation coefficient of 99%). The estimated error was 815.79 which corresponds to 9.2%. The inverted P-impedance volume shows distributed zones of low impedance which can be correlated with prospective reservoirs at some locations within the survey area, away from the wells.

Figure 7 shows the P-impedance inversion result at inline 2524, with inserted P-wave velocity log. The figure shows large lateral and vertical variations in P-impedance along the seismic profile at this inline. Specifically, there is a low-impedance channel at the well location which can be clearly mapped laterally away from the well, in comparison to the input data (Figure 8). The channel is characterized by a varying thickness of sediments

dipping gently in NE-SW direction.



**Figure 6:** Analysis of P-impedance inversion at well W-XXX: Initial P-impedance model log (black); original P-impedance log (blue); inverted P-impedance log (red).



**Figure 7:** P-impedance inversion results at inline 2524. Low-impedance channel is seen which can be clearly mapped laterally.

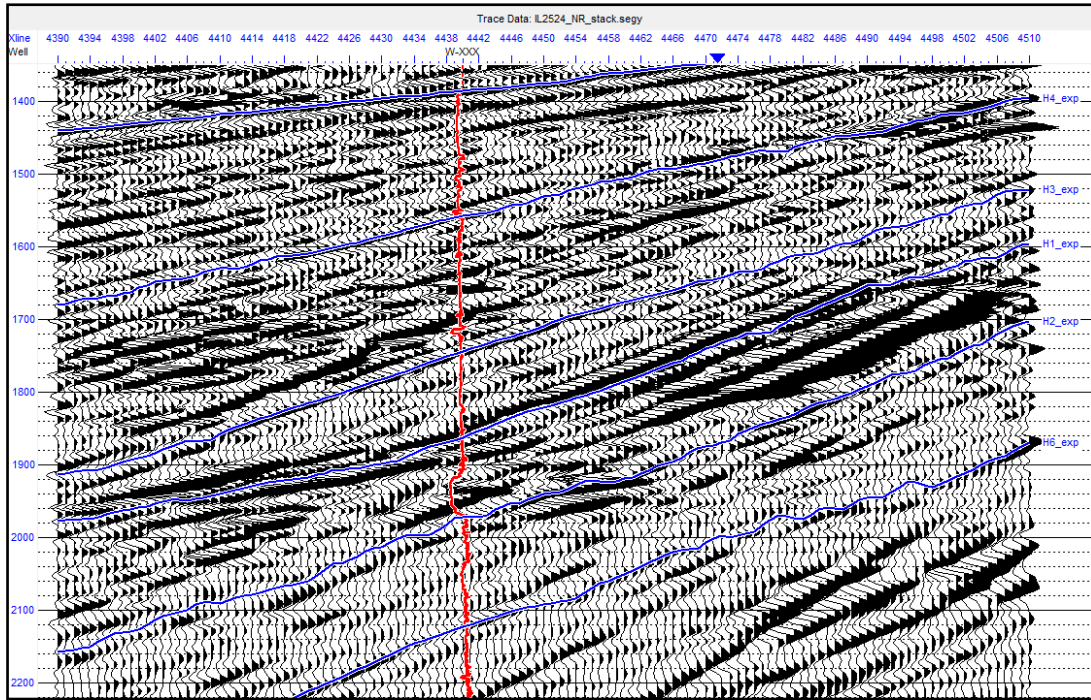


**Figure 8:** Input seismic data at inline 2524 for comparison to inverted P-impedance.

Figure 9 is density volume extracted from the P-impedance volume at inline 2524. The density volume correlates well with the P-impedance volume. Both the P-impedance and density volumes can be analyzed to predict lateral variations in Poisson’s ratio and lithology. P-impedance and/or density reduce(s) as seismic waves encounter gas sands [19], and on the basis of this, the inverted attributes could provide litho-fluid information within existing reservoirs, and also aid in delineating potential reservoirs away from well control.

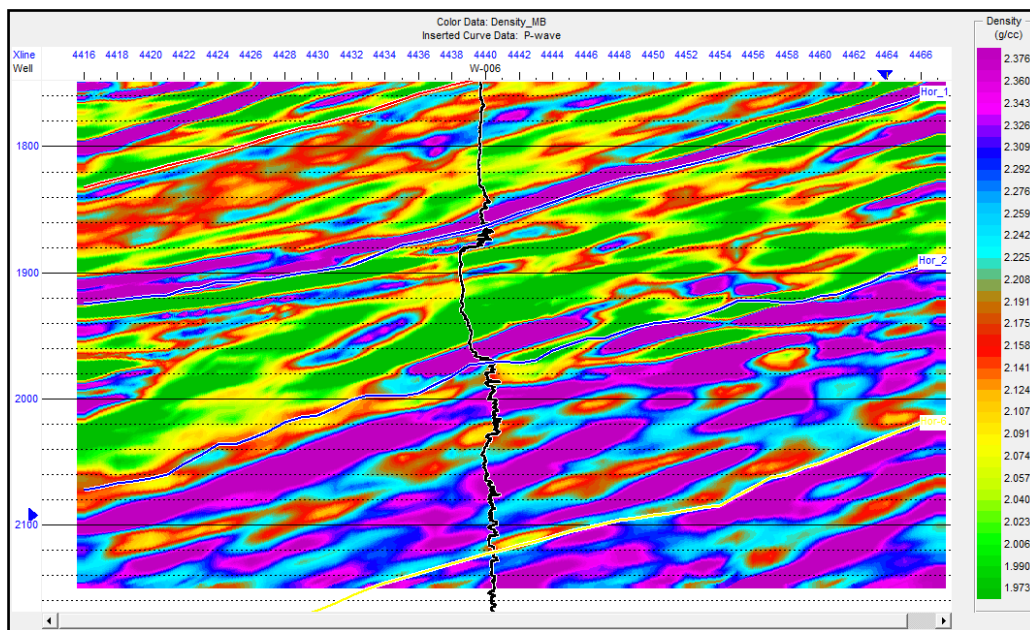


**Figure 9:** Density volume at inline 2524 extracted from P-impedance volume.

#### **4. Conclusion**

Effort was made in this study to invert post stack 3D seismic data acquired in an offshore area in the Niger Delta for acoustic impedance in an attempt to characterize lateral variations in rock property in the area. P-wave velocity and density log data provided the low-frequency input for the inversion to improve data bandwidth, as seismic data is band-limited and does not contain the low frequencies. The results show that acoustic impedance inversion is a veritable tool for delineation of lateral variations in rock property(ies). The method is capable of revealing distributed zones of low acoustic impedance which can be correlated with prospective reservoir zones away from the wellbore. The process reverses the convolution of the source wavelet and earth's reflectivity in order to obtain the impedance and this has the additional advantage of reducing tuning [20] in the data to improve its fidelity. In comparison to the input seismic, the inversion results greatly improve reservoir property interpretability with possible integration with seismic stratigraphy.

#### **Acknowledgements**

The authors are grateful to CGG Geosoftware for providing the software used for the study.

#### **References**

- [1]. R.B. Latimer, R. Davinson, and P. Van Riel, P., An interpreter's guide to understanding and working with seismic derived acoustic impedance data, *The Leading Edge*, 242-256, 2000.
- [2]. P. Veeken, and M. Da Silva, Seismic inversion methods and some of their constraints, *First Break*, 22, 47-70, 2004.
- [3]. C. Wagner, A. Gonzalez, V. Argawal, A. Koesoemadinata, D. Ng, S. Trares, N. Biles, and K. Fisger, Quantitative application of post stack acoustic impedance inversion to subsalt reservoir development, *The Leading Edge*, 528-537, 2012.
- [4]. J. Pendrel, Seismic inversion – the best tool for reservoir characterization, *CSEG Recorder*, 26(10), 18-24, 2001.
- [5]. R.O. Lindseth, Synthetic sonic logs: a process for stratigraphic interpretation, *Geophysics*, 44, 2-26, 1979.
- [6]. M. Becquey, M. Lavegne and C. Willem, Acoustic impedance logs computed from seismic traces, *Geophysics*, 44, 1485-1501, 1979.
- [7]. S. Levy, and P.K. Fullagar, Reconstruction of a sparse spike train from a portion of its spectrum and application to high-resolution deconvolution, *Geophysics*, 46, 1235-1243, 1981.
- [8]. C. Walker and T.J. Ulrych, Autoregressive recovery of the acoustic impedance, *Geophysics*, 48, 1338- 1350, 1983.

- [9]. D.A. Cooke and W.A. Schneider, Generalized inversion of reflection seismic data, *Geophysics*, 48, 665-676, 1983.
- [10]. D. Hampson and B. Russell, First break interpretation using generalized linear inversion, *Journal of the Canadian Society of Exploration Geophysicists*, Vol 20(1), p. 40-54, 1984.
- [11]. Hampson-Russell Ltd., *The theory of Strata program*, Hampson-Russell Ltd, 1999.
- [12]. I. Herawati. "The use of time-lapse p-wave impedance inversion to monitor CO<sub>2</sub> flood at Weburn, Saskatchewan", M.Sc. Thesis, Colorado School of Mines, 2002.
- [13]. L. Keumsuk, Y. Dong-Geun, M. George, H. Namsoon, and H.L. Gwang, A two-dimensional post stack seismic inversion for acoustic impedance of gas hydrate bearing deep-water sediments within the continental slope of the Ulleung Basin, East Sea, Korea, *Terr. Atmos. Ocean. Sci.*, Vol. 24, No. 3, 295-310, 2013.
- [14]. D.W. Oldenburg, T. Scheuer, and S. Levy, S., Recovery of the acoustic impedance from reflection seismograms, *Geophysics*, 48, 1318-1337, 1983.
- [15]. H. Doust, *Petroleum Geology of the Niger Delta*, Geochemical Society, London, Special Publications, 50:365, 1990.
- [16]. K.C. Short, and A.J. Stauble, *Outline of Geology of Niger Delta*. American Association of Petroleum Geologists Bulletin, 67;51:761-779, 1967.
- [17]. E.J. Frankl, E.A. Cordry, *The Niger Delta oil Province: Recent development, onshore and offshore Mexico City*. Seventh world petroleum congress proceedings 2, p. 195-209, 1967.
- [18]. A.A. Avbovbo, *Tertiary Lithostratigraphy of Niger Delta*. American Association of Petroleum Geologists Bulletin, Vol. 62, p.295-306, 1978.
- [19]. A.K. Dubey and I.I.T. Kharagpur, Reservoir characterization using AVO and seismic inversion techniques, 9<sup>th</sup> Biennial International Conference & Exhibition on Petroleum Geophysics, Hyderabad, 2012.
- [20]. R.J.L. Lorenzen, "Inversion of multicomponent time lapse seismic data for reservoir characterization of Vacuum Field, New Mexico", Ph.D Thesis, Colorado School of Mines, 2000.